IMPROVED BURGERS RHEOLOGICAL MODEL AND IDENTIFICATION OF RHEOLOGICAL PARAMETERS FOR SANDY SOFT SOIL UNDER SEEPAGE CONDITIONS

Longbin LIN[1], Hua HU[2*], Zhifeng WU[3]

To investigate the rheological characteristics of soft soil under the influence of seepage, this study focused on sandy soft soil from a deep foundation pit. A series of multi-stage loading triaxial shear rheological tests were conducted after subjecting the soil to different seepage pressures and durations. Based on the rheological curves obtained from the experiments, it was found that the traditional Burgers model provides a good fit at low stress levels but fails to accurately describe the nonlinear rheological behavior at high stress levels. To address this, an improved Burgers rheological model was established by replacing the linear spring element in the original model with a nonlinear spring whose elastic modulus varies with seepage pressure (P) and seepage time (T). The fitting results demonstrate that the new model can more accurately characterize the nonlinear viscoelastic deformation behavior of soft soil under the coupled effects of seepage and stress. This research provides a theoretical basis for revealing the rheological mechanism of soft soil under seepage conditions and for predicting its long-term deformation.

Key words: Seepage shear rheological test; Seepage pressure; Seepage time; Seepage rheological model; Rheological parameters

1. Introduction

Soft rock and soil are widely distributed in the coastal and alluvial regions of China. Under heavy rainfall or groundwater seepage, these weak geomaterials experience microstructural changes and reductions in shear strength, leading to accelerated rheological deformation and potential instability [1]. Understanding their seepage–rheological behavior is thus critical for predicting geotechnical failures and ensuring the safety of major engineering projects.

Existing research mainly focus on four aspects:

[1] Xiamen University Tan Kah Kee College, Fujian, Fujian Zhangzhou,363105, China, email: llb@xujc.com
[2*] School of Architecture and Civil Engineering, Xiamen University, Fujian Xiamen, 361005, China, Xiamen University Tan Kah Kee College, Fujian, Fujian Zhangzhou,363105, China, (corresponding author) email: xmhuh@xmu.edu.cn
[3] Xiamen University Tan Kah Kee College, Fujian, Fujian Zhangzhou,363105, China, School of Architecture and Civil Engineering, Xiamen University, Fujian Xiamen, 361005, China, email: 1191636280@qq.com

First, improvement of soft soil and regulation of rheological properties. Haji and Mir [2] enhanced soil strength using nano-gypsum and cement, while Dubey et al. [3] showed xanthan gum significantly improves erosion resistance. Yaghoubi et al. [4] compared geopolymers and Portland cement for soft clay treatment, and Tran-Nguyen et al. [5] examined permeability characteristics of soil–cement mixtures. These works provide material-based strategies for controlling seepage and rheology.

Second, Constitutive models and rheological theory. Wang et al. [6] described dynamic consolidation of saturated clay with a fractional-order Kelvin model. Frenelus and Peng [7] proposed a visco-elasto-plastic model for deep-buried soft rock, and Liu et al. [8] introduced a fractional-order viscoplastic model considering temperature effects. Wang et al. [9] extended the Burgers creep equation to predict landslide stability. These studies advanced rheological theory but only partially address seepage–time coupling.

Third, Coupled seepage–rheology mechanisms and experiments.Li et al. [10] analyzed phyllite creep damage and permeability under coupled seepage–stress conditions. Puttiwongrak et al. [11] simulated pore pressure effects on soft-soil stability, and Wang et al. [12] examined cyclic seepage–rheology responses in saturated soil. Li et al. [13] developed a damage model for sandstone creep under varying seepage pressures, and Li et al. [14] proposed a shear–creep–seepage model for shale. These studies deepened understanding of multi-field coupling effects.

Fourth, numerical simulation and engineering applications. Hu and Rostami [15] optimized soil rheology during shield tunneling via CFD simulation. Subramaniam and Banerjee [16] analyzed plate-anchor behavior under cyclic loading, while Nourani et al. [17] applied soft-computing models to estimate seepage and stability. Attari et al. [18] studied pile-induced seepage–rheology interactions and the strain-softening risk of sensitive soft soil. These studies offer key methods for controlling seepage, predicting deformation, and ensuring engineering stability.

In summary, although significant progress has been made, research on coupled seepage–rheological testing of soft soil remains limited. Constitutive models that fully incorporate seepage pressure and time effects are still insufficient. Therefore, this study analyzes the influence of seepage on soft-soil rheology, proposes an improved Burgers seepage–rheological model, and validates its rationality and accuracy through comparison with the traditional Burgers model.

2. Seepage-Shear Rheological Test of Sandy Soft Soil under Seepage Conditions

2.1 Sample Collection and Specimen Preparation

The samples were collected from a deep foundation pit in Zhangzhou, Fujian. The strata within the excavation area mainly consist of: (1) miscellaneous fill, (2) silt (containing medium-fine sand), (3) medium-fine sand, (4) silt (containing medium-fine sand), (5) medium-coarse sand, (6) pebbles, (7) completely weathered granite, (8) highly weathered granite, and (9) moderately weathered granite. The hydrogeological conditions of the site are complex, with groundwater recharge primarily from atmospheric precipitation and infiltration of surrounding wastewater, resulting in a multi-layered groundwater system. Under seepage conditions, the rheological characteristics of the silt layers containing medium-fine sand ((2) and (4)) have a particularly significant impact on the deformation and stability of the foundation pit. Representative sandy soft soil samples were collected on-site from the deep foundation pit. The soil appeared black or brownish-gray and was in a semi-liquid-plastic state, naturally saturated. Particle size analysis indicated that the soft soil is mainly composed of a mixture of silt and clay particles, with the proportion of fine or medium-fine sand ranging from 20% to 30%. The natural water content ranged from 48.4% to 58.5%, the average density was 1.58 g/cm^3, and the natural void ratio was between 1.38 and 1.74.

The tests were conducted in accordance with the current "Standard for Geotechnical Testing Method" (GB/T 50123-2019). First, the collected sandy soft soil samples were dried in an oven at 105°C. The dried samples were then crushed, mixed with water, and uniformly adjusted to a water content of 30%. They were sealed and stored for 12 hours to ensure uniform moisture distribution, thereby avoiding interference from water content variations on the test results. Standard sample preparation tools were used to create remolded specimens with dimensions of Ø39.1× 80 mm. A four-layer compaction method was used for specimen preparation, with each layer being vibrated and compacted to ensure uniform density.

2.2 Triaxial Shear Rheological Test Scheme for Sandy Soft Soil under Seepage Conditions

2.2.1 Loading Method for Rheological Test

Indoor rheological tests on soft soil can be conducted using two methods: separate loading and multi-stage loading. Separate loading requires the preparation of multiple identical specimens to be tested rigorously and

simultaneously under identical equipment and conditions but with different loads. In contrast, multi-stage loading involves progressively increasing the load stress on a single specimen. The resulting stepped strain-time curve is then processed using Chen's method to obtain the rheological curves for each load level acting individually [19]. Multi-stage loading can avoid the absolute errors that arise from preparing different specimens and simplifies the experimental procedure. Therefore, the multi-stage loading method was chosen for the rheological tests.

2.2.2 Preliminary Triaxial Shear Exploration Tests

In deep foundation pit engineering, sandy soft soil is prone to seepage-rheological deformation and failure under the combined effects of seepage and gravitational loads. The influencing factors include seepage conditions, the physical and mechanical properties of the soil, and the stress environment of the soil. Seepage conditions include seepage time and seepage pressure. The soil's stress environment includes external loads and confining pressure. To more accurately simulate the entire process of seepage-rheological failure in the specimens, it is necessary to scientifically and reasonably determine experimental parameters such as confining pressure and the magnitude of multi-stage loading. To this end, consolidated drained triaxial shear tests were first conducted on the specimens under different confining pressures of 50 kPa, 120 kPa, and 180 kPa. The shear rate was set at 0.05 mm/min. Failure was determined when the strain reached 16% or the deviator stress peaked. This allowed for obtaining the stress-strain curves for shear failure under different confining pressures and determining the peak shear strength of the specimens, which provided a basis for setting the subsequent load values. Fig. 1 shows the stress-strain relationship curve of a representative specimen and the photograph of the triaxial shear testing apparatus.

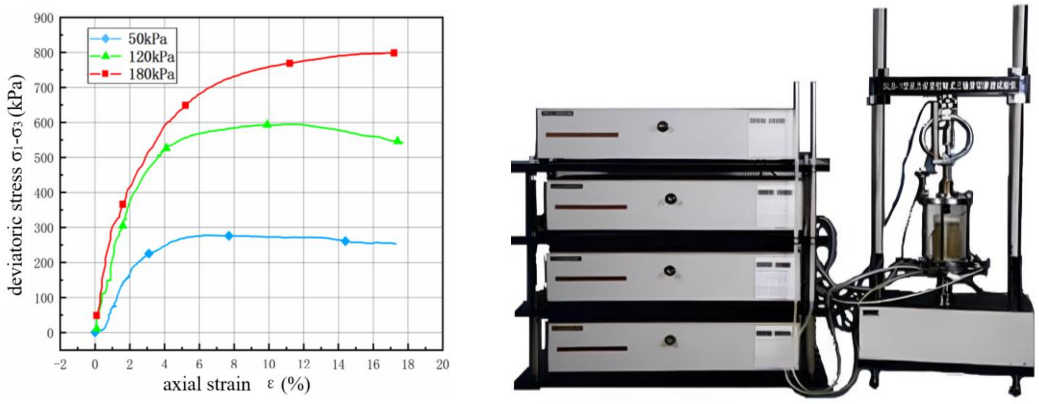

(a)Stress-strain relationship curve (b) SLB-1 Triaxial Seepage–Shear Apparatus for Stress–Strain Testing

Fig. 1. Consolidated drained triaxial shear test results and schematic diagram of the apparatus

2.2.3 Triaxial Shear Rheological Test Scheme for Sandy Soft Soil under Seepage Conditions

The experiment was conducted using an SLB-1 stress-strain controlled triaxial seepage-shear test apparatus from Nanjing Soil Instrument Factory Co., Ltd. This apparatus offers two seepage control modes: constant pressure difference and constant flow rate, enabling triaxial shear tests and triaxial seepage-rheological tests under seepage conditions. The instrument can create precise and stable seepage pressure conditions by setting the water inlet pressure and drainage back pressure at both ends of the specimen to establish a constant seepage pressure difference.

Based on the peak shear strength values from the failure tests, and considering the operational parameters and performance of the test apparatus, the experimental scheme maintained a constant confining pressure of 180 kPa. The specimens were first subjected to seepage and then underwent the triaxial shear rheological test. The rheological test used a four-stage loading method, with load levels of 150 kPa, 300 kPa, 450 kPa, and 600 kPa, respectively. At each loading stage, if the specimen's rheological deformation stabilized without failure, the next loading stage of the rheological test was applied until the specimen experienced rheological failure. The selection of seepage parameters for the experiment needed to consider the range of variations caused by groundwater in the foundation pit or different rainfall levels. For this experiment, seepage pressures of 10 kPa, 30 kPa, 50 kPa, and 70 kPa were selected, while seepage durations of 48 min, 72 min, 96 min, and 120 min were chosen. The tests used remolded, saturated sandy soft soil specimens with identical water content; therefore, the influence of water content was not a factor in the experimental design. To compare the rheological parameters of a specimen without the effect of seepage, specimen No. 17 was specifically added. The shear rheological test scheme under seepage conditions is shown in Table 1.

Table 1

Triaxial Shear Rheological Test Scheme for Soft Soil Samples with Sand under Seepage Conditions

Specimen No.	Seepage Pressure P/kPa	Seepage Time T/min	Specimen No.	Seepage Pressure P/kPa	Seepage Time T/min
1	10	48	10	50	72
2	10	72	11	50	96
3	10	96	12	50	120
4	10	120	13	70	48
5	30	48	14	70	72
6	30	72	15	70	96
7	30	96	16	70	120
8	30	120	17	0	0
9	50	48			

2.3 Triaxial Seepage-Shear-Rheological Test

The specimen was installed according to the test specifications. A constant confining pressure of 180 kPa was applied. After the completion of drained consolidation, test parameters such as inlet water pressure and outlet back pressure were set at both ends of the specimen to create a seepage pressure across it via the pressure difference. First, the specimen was subjected to seepage. After the preset seepage time was reached, the test automatically transitioned to a drained shear rheological test. Following the four-stage loading rheological test plan, the duration for each load level was set to 180 minutes, or until the rheological deformation tended to stabilize, at which point the next load level was applied to continue the test. The deviatoric stress was applied step by step, allowing the soil sample to undergo full rheological deformation under each load level. When the axial rheological strain reached 16%, the specimen was considered to have met the failure criterion, and the test was automatically terminated. Throughout the test, various data points such as rheological time, axial deviatoric stress load, and axial rheological strain were automatically recorded and saved, generating curves like the axial rheological strain versus rheological time. According to the test plan, a total of 17 specimens underwent four-stage loading, resulting in a total of 68 rheological tests.

3. Results and Analysis of Triaxial Seepage-Shear Rheological Tests under Seepage Conditions

3.1 Four-Stage Rheological Curves and Characteristic Analysis after Processing with Chen's Method

Chen's method, established by Professor Chen Zongji, primarily consists of two parts: a step-loading technique and a data processing system. This method utilizes a step-loading model on a single specimen and incorporates the superposition principle, which considers the material's memory effect, to convert the rheological curve under multi-stage stress into an equivalent single-stage loading response curve, as shown in Fig. 2. Compared to traditional separate loading tests, this method significantly reduces the impact of specimen variability on the assessment of long-term strength and rheological models, while also shortening the testing period and reducing resource consumption.

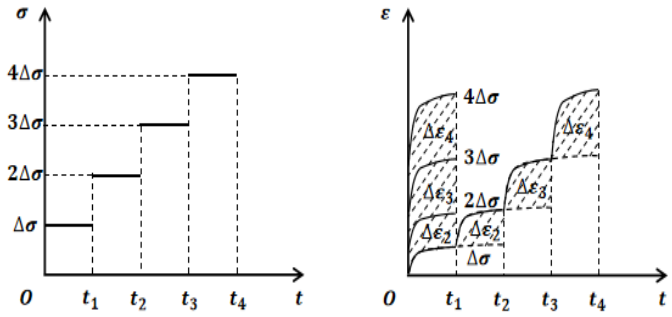

(a) Diagram of four-stage loading (b) Strain-time relationship curve

Fig. 2. Schematic diagram of Chen's multi-stage loading method[20]

Based on the four-stage loading rheological tests, rheological curves under four load levels were obtained. Using Chen's processing method, the rheological curves under multi-stage loading were converted into equivalent single-stage loading rheological curves. Due to space limitations, Fig. 3 only shows the four-stage rheological curves for specimens 1-4 after being processed by Chen's method.

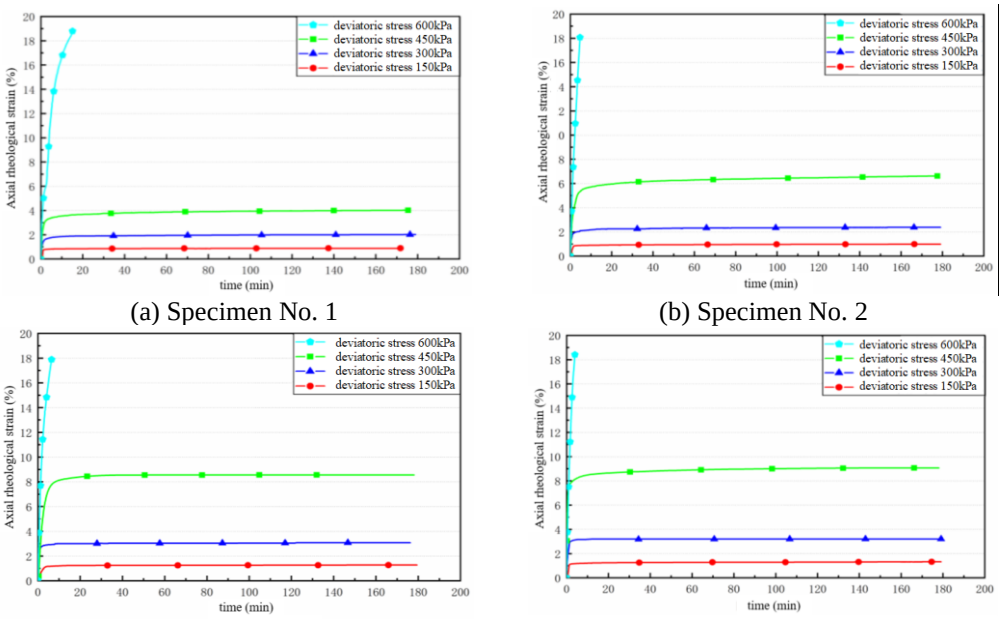

(a) Specimen No. 1 (b) Specimen No. 2

(c) Specimen No. 3 (d) Specimen No. 4

Fig. 3. Four stage rheological curves of samples 1-4 after Chen's method treatment under a confining pressure of 180kPa

By summarizing and analyzing the collected experimental data and the rheological curves of the specimens, the following common rheological characteristics were identified:

(1) The specimens all exhibited a significant elastic deformation response, manifested as an instantaneous surge in strain, during the initial phase of load increase. As the load was sustained, the specimens entered a nonlinear viscoelastic rheological stage, where their strain development showed typical attenuation characteristics, meaning the strain growth rate continuously decreased [21]. Finally, the rate stabilized at a low level as the specimens entered the steady-state creep phase.

(2) Under otherwise identical conditions, the increase in rheological strain was positively correlated with the increase in the deviatoric stress load level. As the deviatoric stress level increased, the rheological deformation gradually became larger, and the magnitude of the increase also expanded.

(3) When the deviatoric stress load level was low, specifically less than 0.5 times the failure deviatoric stress, the deformation of the specimen was mainly instantaneous elastic strain, and the axial rheological deformation was relatively insignificant. As time progressed, the specimen transitioned to a slow rheological deformation, and the curve gradually flattened, eventually becoming almost parallel to the time axis, indicating that the rheological strain was approaching a stable limit.

(4) Due to the effect of seepage, the specimen's internal shear strength parameters, such as cohesion and the angle of internal friction, were reduced, leading to a decrease in peak shear strength. Consequently, when the load was increased to the fourth level of 600 kPa, the rheological strain in the specimens increased rapidly, quickly reaching the failure strain value, which manifested as the failure stage of accelerated rheological deformation.

3.2 Traditional Burgers Rheological Model and Parameter Identification

3.2.1 The Traditional Burgers Rheological Model

The traditional Burgers model [22] is a classic linear viscoelastic model composed of a Maxwell unit and a Kelvin unit connected in series. It can describe a material's instantaneous elastic deformation response, delayed elastic deformation response, and viscous deformation characteristics, and it is widely used in the study of soft soil rheology. The traditional Burgers rheological model is shown in Fig. 4.

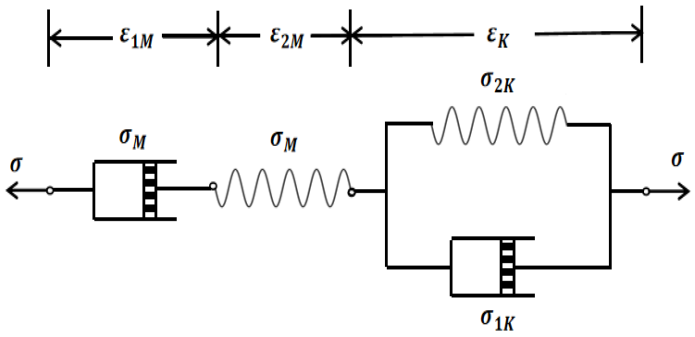

Fig. 4. Traditional linear viscoelastic Burgers rheological model

According to the stress-strain laws for series and parallel connections of element models, the rheological equation for the traditional Burgers model is:

$$\varepsilon = \sigma\left[\frac{1}{E_M} + \frac{t}{\eta_M} + \frac{1}{E_K}\left(1 - e^{-\frac{E_K}{\eta_K}t}\right)\right] \tag{1}$$

In the rheological model, the subscripts M and K represent the Maxwell and Kelvin parts of the model, respectively. In the rheological equation, σ is the total stress load (kPa), ε is the total rheological strain (%), t is the rheological time (min), EM is the instantaneous elastic modulus (kPa), EK is the delayed elastic modulus (kPa), ηM is the instantaneous viscosity coefficient (Pa·s), and ηK is the delayed viscosity coefficient (Pa·s).

3.2.2 Fitting Analysis of Rheological Curves with the Traditional Burgers Model

When using the traditional Burgers viscoelastic model to fit the experimental curves, it was found that the model provided a good fit for the rheological curves of the specimens under the first and second (low stress) load levels. However, under high-stress loading, the predicted rheological curves deviated significantly from the experimental results. The reason for this is that the traditional Burgers model falls within the theoretical framework of linear rheology. Under the influence of seepage, water flow alters the microstructure of the soil through physical, chemical, and mechanical actions. This enhances the softening, mud-making, and dissolution effects in the soil, leading to a loss of cementation between particles, a reduction in internal cohesion and the angle of internal friction, and a sharp decrease in shear strength. The mechanical properties degrade, and the elastic modulus changes accordingly, promoting rapid rheological deformation and making nonlinear rheological characteristics more pronounced [23]. Therefore, using the traditional linear viscoelastic Burgers model to fit the rheological curves inevitably leads to significant errors.

4. The Improved Burgers Seepage-Rheological Model and Parameter Identification

4.1 The New Improved Burgers Seepage-Rheological Model

To better describe the nonlinear viscoelastic rheological characteristics of the specimens, the two linear spring elements in the traditional model were replaced with nonlinear spring elements. Their corresponding elastic moduli are defined to vary as a quadratic polynomial function of two variables: seepage pressure (P) and seepage time (T). During the seepage process, the effect of seepage on the water content of the specimens is not significant, and thus the change in the specimens' viscosity coefficients is minimal. Therefore, the instantaneous viscosity coefficient and the delayed viscosity coefficient are kept constant, resulting in the modified Burgers seepage-rheological model shown in Fig. 5.

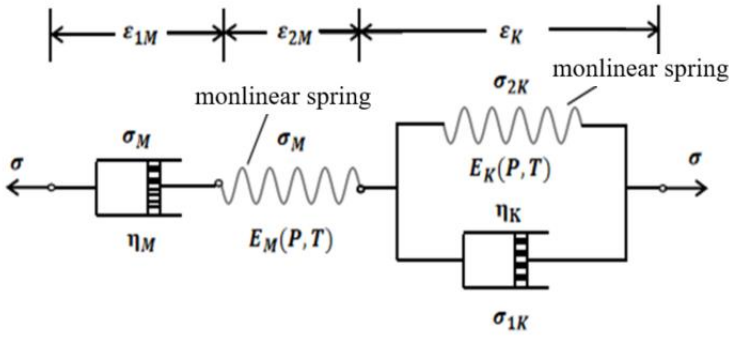

Fig. 5. Modified Nonlinear Viscoelastic Burgers Seepage Rheological New Model

In this model, the instantaneous elastic modulus (EM) and the delayed elastic modulus (EK) are adjusted to be quadratic polynomial functions. Using the LinearRegression class from the Python machine learning library scikit-learn, the quadratic functional expressions for EM and EK were obtained through fitting. This quadratic polynomial consists of four parts: the first is a constant term, the second includes first-order terms for single factors, the third includes second-order terms for single factors, and the fourth includes second-order terms for the interaction between different factors, as shown in Equations (2) and (3). By combining Equations (1), (2), and (3), the new nonlinear viscoelastic seepage-rheological equation for sandy soft soil, incorporating seepage parameters, is established.

$$E_M = E_{M0} + \alpha_1 x_1 + \alpha_2 x_2 + \alpha_{11} x_1^2 + \alpha_{22} x_2^2 + \alpha_{12} x_1 x_2 \tag{2}$$

$$E_K = E_{K0} + \beta_1 x_1 + \beta_2 x_2 + \beta_{11} x_1^2 + \beta_{22} x_2^2 + \beta_{12} x_1 x_2 \tag{3}$$

where x1 is the seepage pressure P (kPa), x2 is the seepage time T (min); α1, β1, α2, β2 are the first-order coefficients; α11, β11, α22, β11, α12, β12 are the

second-order coefficients; EM is the instantaneous elastic modulus under seepage conditions (kPa), EM0 is the instantaneous elastic modulus under no-seepage conditions (kPa), EK is the delayed elastic modulus under seepage conditions (kPa), and EK0 is the delayed elastic modulus under no-seepage conditions (kPa).

4.2 Parameter Identification for the Improved Burgers Seepage-Rheological Model

The LinearRegression class function from the Python machine learning library scikit-learn was used to fit and identify EM and EK. The principle behind this is to estimate the model parameters using the method of least squares. For this study, the rheological curves from the first three non-failure loading stages of specimens 5-16 were used as the sample for parameter fitting and regression, while specimens 1-4 were reserved for a comparative validation between the new model and the traditional model. The parameter fitting and identification for the model were automated through programming. The identified fitting parameters for EM and EK are shown in Table 2. The coefficients of determination (R2) were 0.9936 and 0.9903, respectively. EM0 and EK0 are the fitted values from the rheological test results of specimen No. 17 under no-seepage conditions.

Table 2

Calculation of fitting coefficients for EM and EK of samples 5-16

E_M	E_{M0}	α_1	α_2	α_{11}	α_{22}	α_{12}
Fitted Value	447.3	-1.4975	-1.7605	0.0061	0.0097	-0.019
E_K	E_{K0}	β_1	β_2	β_{11}	β_{22}	β_{12}
Fitted Value	485.9	-3.8255	-1.0381	0.0285	0.0024	-0.0118

Thus, the quadratic functional expressions for the elastic moduli in the improved seepage-rheological model are:

$$E_M = 447.3 - 1.4975x_1 - 1.7605x_2 + 0.0061x_1^2 + 0.0097x_2^2 - 0.019x_1x_2 \quad (4)$$

$$E_K = 485.8763 - 3.8255x_1 - 1.0381x_2 + 0.0285x_1^2 + 0.0024x_2^2 - 0.0118x_1x_2 \quad (5)$$

5. Comparison of Fitting Performance between the Original and Modified Burgers Seepage-Rheological Models

Using specimens 1, 2, 3, and 4 as examples, the improved seepage-rheological model and its parameters were imported into Origin software. The fitting results from the traditional Burgers model, the fitting results from the modified Burgers seepage-rheological model, and the experimental rheological curves were plotted together for comparison, as shown in Fig. 6. As seen in the figures, at low stress levels, the predicted curves from both the traditional Burgers

model and the modified Burgers seepage-rheological model are closely aligned with the experimental curves. However, under high stress conditions, the predicted curve from the traditional Burgers model deviates significantly from the experimental curve, whereas the improved Burgers seepage-rheological model can still predict the actual rheological curve very well. Due to the limited number of tests, random experimental errors caused small deviations between the predicted and experimental curves for a few specimens. For instance, the difference between the predicted and experimental rheological curves for specimen 3 under the third load level was approximately 1%. Overall, however, the performance of the improved Burgers seepage-rheological model in describing the seepage-rheological curves of soft soil is far superior to that of the traditional Burgers model. This demonstrates that the new improved model is scientifically sound, rational, accurate, and effective.

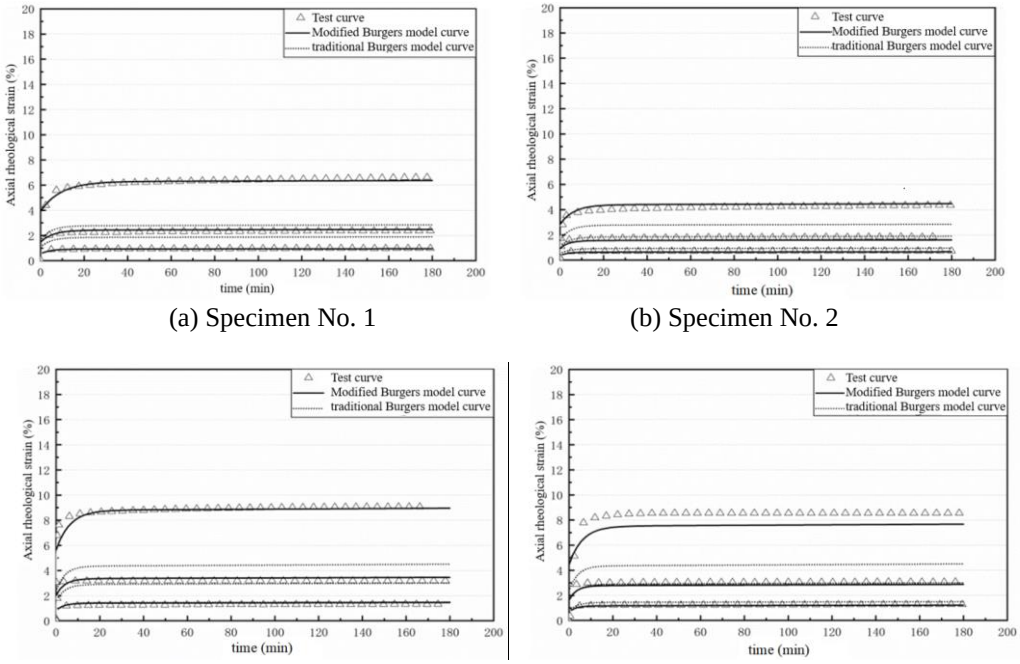

(a) Specimen No. 1 (b) Specimen No. 2

(c) Specimen No. 3 (d) Specimen No. 4

Fig. 6. Comparison of Error between Modified Seepage Rheological New Model, Traditional Model Fitting Rheological Curve and Actual Rheological Curve

6. Conclusions

This study significantly improved the prediction accuracy of the rheological behavior of sandy soft soil under seepage conditions by constructing a nonlinear Burgers model that couples the dual factors of seepage pressure and time. The experimental and fitting results consistently show that the traditional linear Burgers model has significant limitations at high stress levels because it

does not account for the modulus degradation and structural softening caused by seepage. The improved model, by introducing a quadratic functional relationship where the elastic modulus varies with seepage parameters (P, T), accurately describes the nonlinear viscoelastic deformation stage, with its coefficient of determination ($R^2 > 0.99$) being significantly superior to the traditional method. This advancement not only deepens the understanding of the rheological mechanism of soft soil under the coupled effects of seepage, stress, and time but also provides a more reliable mathematical model for long-term deformation prediction and stability control in engineering practice.

However, this research was based on laboratory remolded specimens and constant seepage pressure conditions, which may not fully reflect the structural nature of natural soil and the complexity of in-situ seepage paths. It is recommended that future research incorporate in-situ monitoring data to conduct model validation and parameter sensitivity analysis under multi-field coupling conditions. Furthermore, the potential of methods such as machine learning for rheological parameter inversion and model optimization should be explored.

Acknowledgement

This work was supported by the National Natural Science Foundation of China (Grant No. 51278437), the Xiamen Natural Science Foundation Project (Grant No. 3502Z20227323), and projects from the Department of Housing and Urban-Rural Development of Fujian Province (Grant Nos. 2023-K-79, 2023-K-75).

R E F E R E N C E S

[1] *Hu H,Wu X*. Triaxial test study on influence of confining pressure and osmotic pressure on shear strength of granite residual soil. Journal of Xiamen University (Natural Science), 2021, 60(04): 762-766.

[2] *Haji T R, Mir B A*. Effect of nano-gypsum on mechanical properties cement admixed marginal silty soil. Construction and Building Materials, 2023, 408: 133639.

[3] *Dubey A A, Machale J, Ravi K, et al*. Rheological properties of xanthan-gum solutions and their role in improving river embankments. Geotechnical and Geological Engineering, 2024, 42(4): 2387-2401.

[4] *Yaghoubi M, Arulrajah A, Horpibulsuk S.* Engineering behaviour of a geopolymer-stabilised high-water content soft clay. International Journal of Geosynthetics and Ground Engineering, 2022, 8(3): 45.

[5] *Tran-Nguyen H H, Luong B T, Nguyen K D T.* Investigation of the hydraulic conductivity of soilcrete specimens made by soft clays and medium clays mixed with cement. Geotechnical and Geological Engineering, 2023, 41(2): 1073-1082.

[6] *Wang L, Chen H, Liu S, et al.* Rheological consolidation analysis of saturated clay ground under cyclic loading based on the fractional order Kelvin model. International Journal for Numerical and Analytical Methods in Geomechanics, 2024, 48(7): 1814-1832.

[7] *Frenelus W, Peng H*. Evaluating the time-dependent behavior of deeply buried tunnels in soft rock environments and relevant measures guaranteeing their long-term stability. Applied Sciences, 2023, 13(18): 10542.
[8] *Liu G, Chen Y, Rim H C, et al.* Viscoplastic solutions of time-dependent deformation for tunnels in swelling rock mass considering stress release. Journal of Rock Mechanics and Geotechnical Engineering, 2023, 15(8): 2053-2071.
[9] *Wang S, Zhan Q, Wang L, et al*. Unsaturated creep behaviors and creep model of slip-surface soil of a landslide in Three Gorges Reservoir area, China. Bulletin of Engineering Geology and the Environment, 2021, 80(7): 5423-5435.
[10] *Li T, Peng F, Chen C, et al*. Investigating the creep damage and permeability evolution mechanism of phyllite considering Non-Darcy's flow. Rock Mechanics and Rock Engineering, 2024, 57(10): 8483-8498.
[11] *Puttiwongrak A, Deekaoropkun T, Sin K P, et al.* Basal Heave Stability Analysis of Excavations in Bangkok Soft Clay with Confined Groundwater Recovery Using Numerical Modeling[J]. Modelling, 2025, 6(1).
[12] *Wang S, Cai Y, Zhang L, et al*. Experimental study on dynamic characteristics of saturated soft clay with sand interlayer under unidirectional and bidirectional vibration. Buildings, 2023, 13(10): 2534.
[13] *Li Y, Song Y, Huang D*. Creep behavior and damage constitutive model of sandstone: an experimental study on seepage-load coupling. Mechanics of Time-Dependent Materials, 2024, 28(4): 2751-2770.
[14] *Li G, Wang Y, Wang D, et al*. The creep behavior of rock shear seepage under different seepage-water pressures. Mechanics of Time-Dependent Materials, 2023, 27(2): 351-365.
[15] *Hu W, Rostami J.* A new method to quantify rheology of conditioned soil for application in EPB TBM tunneling. Tunnelling and Underground Space Technology, 2020, 96: 103192.
[16] *Subramaniam R, Banerjee S.* Three-Dimensional Numerical Analysis of Static and Cyclic Pull-out Response of Plate Anchors in Reinforced Soft Clay. International Journal of Geosynthetics and Ground Engineering, 2024, 10(3): 46.
[17] *Nourani V, Behfar N, Dabrowska D, et al.* The applications of soft computing methods for seepage modeling: A review. Water, 2021, 13(23): 3384.
[18] *Attari Y, Jostad H P, Grimstad G, et al*. Evaluation of Pile Driving Effe cts on Slope Stability in Clay. Geotechnical and Geological Engineering, 2024, 42(3): 1623-1638.
[19] *Liu JF, Li S, Duan GJ, et al*. Phase transition properties and rheological model of soft clay in South China Sea in steady rheological tests. Rock and Soil Mechanics, 2023, (S1): 341-349.
[20] *Li W*. Study on Cfrd Long-term Deformation Law with Deep Alluvium Considering Seepage-creep Coupling Effect. Xi'an university of Technology, 2023.
[21] *Du YF, Xia HH, Hu PL, et al.* Experimental Study on Creep Behaviors of Marine Soft Soil in Guangzhou. Journal of Water Resources and Architectural Engineering, 2013, (02): 12-16.
[22] *Josef Málek, Kumbakonam R.Rajagopal, Karel T˚uma*. Derivation of the Variants of the Burgers Model Using a Thermodynamic Approach and Appealing to the Concept of Evolving Natural Confgurations. Fluids, 2018: 3(4): 69.
[23] *Hu H, Cai L, Cheng J, et al.* Experimental Analysis on the Accelerating Rheological Failure Process of Soft Soil Based on the Catastrophe Theory. International Conference on Mechanics and Civil Engineering (icmce 2014), 2014: 635-639.